

Maturation of siRNA by strand separation: Steered Molecular dynamics study

Rakesh K Mishra¹, Sanchita Mukherjee², Dhananjay Bhattacharyya^{*1}

¹ *Computational Science Division, Saha Institute of Nuclear Physics Kolkata, 700064, India.*

² *Department of Biological Sciences and Centre for Climate and Environmental Studies, Indian Institute of Science, Education and Research-Kolkata, Mohanpur 741246, India*

Abstract

RNA interference, particularly siRNA induced gene silencing is becoming an important avenue of modern therapeutics. The siRNA is delivered to the cells as short double helical RNA which becomes single stranded for forming the RISC complex. Significant experimental evidence is available for most of the steps except the process of the separation of the two strands. We have attempted to understand the pathway for double stranded siRNA (dsRNA) to single stranded (ssRNA) molecules using steered molecular dynamics simulations. As the process is completely unexplored we have applied force from all possible directions restraining all possible residues to convert dsRNA to ssRNA. We found pulling one strand along helical axis direction restraining far end of the other strand demands excessive force for ssRNA formation. Pulling a central residue of one strand, in a direction perpendicular to the helix axis, while keeping the base paired residue fixed requires intermediate force for strand separation. Moreover we found that in this process the force requirement is quite high for the first bubble formation (nucleation energy) and the bubble propagation energies are quite small. We hypothesize this could be the mode of action adopted by the proteins in the cells.

I. INTRODUCTION

Ribonucleic acid (RNA) interference (RNAi) was first time discovered in plants, but it was not noted in animals until Fire and Mello demonstrated that double-stranded RNA (dsRNA) can cause greater suppression of gene expression than single-stranded RNA (ssRNA) in *Caenorhabditis elegans* [1]. Due to the excellent gene silencing potential of RNAi, it has attracted broad attention to exploit its capabilities. In recent years, RNAi has become more and more important in gene silencing and drug development because of its high specificity, significant effect, minor side effects and ease of synthesis [2]. When dsRNA enters the cell, it is first cleaved into short double stranded fragments of 20 – 23 nucleotide silencing RNAs. These cleaved products have been recognized as the small interfering RNAs (siRNAs) in the form of double stranded helices. They are generally named as passenger strand and guide strand. Presumably the double helix also remains complexed with RNA-Induced Silencing Complex (RISC). In the RISC, the guide strand of siRNA pairs with a complementary sequence in a messenger RNA (mRNA) molecule and induces cleavage of mRNA by enzyme Argonaute. Thus, the process of mRNA translation can be interrupted by siRNA [3–6]. Since rational design of siRNA can specifically inhibit endogenous and heterologous genes, it can modulate any disease-related gene expression. Following this strategical revelation, several synthetic siRNA are being designed with desirable sequences to inhibit any target gene expression [7–9]. The siRNAs undergo further processing inside the cell, where, one strand or part of one (say guided strand) gets separated from the other strand (say passenger strand). This separation takes place by the force generated by some enzymatic reaction. The naturally coded microRNA (miRNA) also goes through similar steps for their action. Thus, the structure and force involved in the separation of the strands become one of the important aspects to deal with the efficiency of siRNA.

Double-helical deoxyribonucleic acid (dsDNA) has been widely studied with respect to strand separation based on experiments and theory [10–20], where researchers have studied the effects of mechanical force on the structural changes of dsDNA. It has been shown that

differences in the chemical structure of dsDNA and dsRNA molecules affects the intra-strand distances [21]. Recardo *et al.* [22] have studied the effects of force using optical and magnetic tweezers on the stretching of dsRNA and compared it with dsDNA results. Lipfert *et al.* [23] have studied the effects of force and torque on the structural changes of long stretch of dsRNA and pointed out striking differences between dsRNA and dsDNA. Unfolding of compact structure of RNA was also studied recently by various groups using experiment and simulation [24–27].

Nevertheless, siRNA evolves as one of the unprecedented small bio-molecule, unlike large polymeric DNA or various RNA motifs, requiring broad study of structural changes under the application of external mechanical force. Oligomeric siRNA, having 20 to 22 base-pairs and UU overhang in both the strands requires special attention in its structural changes during unzipping. It may be mentioned that natural microRNAs (miRNA) also require unzipping after they are processed by DICER protein, which may require some assistance from proteins. We approach this novel problem of siRNA strand separation by focusing our study on the opening of both the strand of siRNA under the application of external mechanical force. This mechanical force might come from some protein, such as Argonaute, DICER or some other RNA binding protein, within the cell. However, we could not find any report on action of such protein in the literature. It may be noted that partial strand separation of dsDNA also takes place during transcription initiation. It was found that the sigma-factor of RNA polymerase is responsible for that [28–30]. Thus, separation of strands of double helical nucleic acid chains is an important aspect for understanding several biochemical pathways. In this report, we present the effects of the pulling with the constant velocity steered molecular dynamics (SMD) simulations under different protocols as shown in Figure 1, broadly classifying them as axial pulling and unzipping. We provided a comparative study using all atom MD simulation, which may help in characterizing the structural changes that occur during the pulling of double-stranded siRNA. We address the problem with extensive studies of structural parameters, hydrogen bonds (H-bonds) disruption and stacking inter-

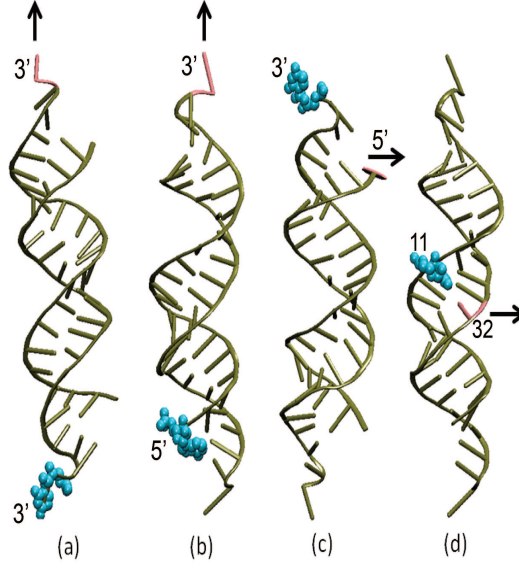


FIG. 1: Schematic diagram showing different protocols studied in this report: (a) Shows the Axial Rupture system, where force is applied along the helical direction. In this case force is applied at 3'-end of one strand keeping 3'-end of its complementary strand fixed. (b) Shows the Axial Stretch model, where force is applied along the axial direction of the system. But, in this case pulling is applied at 3'-end of one strand while 5'-end of the same strand being fixed. (c) Shows Terminal Unzip model, where force is applied perpendicular to the helical direction. In this case, pulling is applied at 5'-end of one strand keeping 3'-end of its complementary strand fixed. Here, both pulling and fixed ends are in the same side of the duplex. (d) Corresponds to the Central Unzip model, where force is applied perpendicular to the helical direction at the central residue of the system.

actions. The present studies, which are involved in calculation of path dependent force and disruption of H-bonds by various protocols may shed the light to provide future perspective of binding proteins with siRNA for gene silencing. The analyses may also be important for designing more effective siRNA sequences.

The paper is organized as follows: in Section II, we describe the computational protocol

for simulation and analysis. Section III contains analysis of the measured force on the strands and the reason behind such forces. In Section IV, we have discussed variation of different structural parameters of the RNA. Section V describes implication of the studies and how our results are consistent with the available experimental data.

II. MODEL AND METHOD

A. Equilibrium MD simulation:

Starting system : Well studied siRNA crystal structure with PDB ID 2F8S [31] is taken for all the simulations. The structure is comprised of 22 nucleotides on each strand of the duplex with characteristic UU overhang in both the 3'-ends. The self-complementary sequence is, 5'(AGACAGCAUAUAUGCUGUCUUU)₂. The dimension of the duplex is \approx 8.0 nm in length in normal double helical form.

Protocol: All molecular dynamics simulations were carried out using GROMACS 5.1 package [32] and CHARMM36 Force Field [33]. The complete siRNA double helical structure, without the Argonaute protein interacting through one end of the RNA, was considered including the 5'-terminal phosphate groups. The siRNA is solvated with TIP3P water model in cubic box with sufficient dimension (10 nm \times 10 nm \times 10 nm) and neutralized with 44 Na⁺ ions. The system is then subjected to energy minimization by steepest descent method to eliminate initial stress. For initial equilibration, standard protocol of 100 ps each of NVT and NPT simulations were done [34]. Position restraints was applied to the RNA atoms during equilibration of the system for both NVT and NPT processes. The siRNA and non siRNA atoms were coupled to separate temperature coupling baths, maintaining 300 K using Berendsen weak coupling method [35]. Final 100 ns NPT production MD run was conducted in absence of any restraints. In the production run, the Nose-Hoover thermostat [36, 37] was used to maintain temperature and the Parrinello-Rahman barostat [36–39] was used to isotropically regulate pressure. Periodic boundary conditions (PBC) were employed for

all simulations and the particle mesh Ewald (PME) method [40] was used for long-range electrostatic interactions. The simulation time step was set to 2 fs with LINKS algorithm to maintain bond lengths involving hydrogen atoms. Final structure from the end of 100 ns equilibrium trajectory was used as starting configurations for pulling simulations.

Steered MD simulation:

Four different steered molecular dynamics simulations (SMD) were carried out with equilibrated conformations of siRNA along with solvents at 300 K. Henceforth we would refer to them as: (i) Axial Rupture, (ii) Axial Stretch, (iii) Terminal Unzip and (iv) Central Unzip. In case of Axial Rupture, shown in Figure 1a, force is applied at the 3'-terminal residue of one chain keeping the 3'-terminal residue of its complementary strand fixed (immobile) to their original position. For Axial Stretch (Figure 1b), we have fixed the 5'-terminal residue of one strand and applied force on the 3'-terminal residue of the same strand along the helical direction of the system. In case of Terminal Unzip, shown in Figure 1c, we have fixed the 3'-terminal residue of one strand and force is applied on the 5'-end of its complementary strand along a direction perpendicular to the helical axis. Here both the 3'- and 5'-terminal residues are in the same side of the double helix. In Central Unzip case (Figure 1d) the force has been applied in the central point (residue 11) of one strand keeping the central residue of the complementary strand fixed. This is also the case, where force is applied perpendicular to the helical direction. In case of pulling simulations, big rectangular boxes with dimensions sufficient to satisfy minimum image convention for complete separation of siRNA were generated. This provided space for the nearly elongated single stranded RNA along the Z-axis for the rupture and along Y-axis (perpendicular to the Z-axis) for the unzipping. We have adopted the boxes of the size 15 nm \times 15 nm \times 54 nm, 15 nm \times 15 nm \times 54 nm, 15 nm \times 40 nm \times 15 nm and 15 nm \times 40 nm \times 15 nm, for Axial Rupture, Axial Stretch, Terminal Unzip and Central Unzip respectively. These boxes were filled with TIP3P model of explicit water with adequate Na⁺ counterions to neutralize the systems. Equilibration was performed for 200 ps NVT and 10 ns NPT simulations, using the same methodology described above prior to SMD simulations.

Protocol:

SMD is based on applying external forces to particles in a selected direction by adding a spring-like restraint, thus imitating directly the basic idea of an AFM experiment through optical or magnetic tweezers. The SMD simulations with constant velocity (CV) stretching (SMD-CV protocol) were carried out by fixing one of the residues and applying external forces to the dummy atoms attached to center of mass of another residue (SMD residue) with a virtual spring. After several test simulations, we adopted a spring constant value of $1000 \times kJ \times mol^{-1} \times nm^{-2}$ and a pulling rate of $0.0008 \times nm \times ps^{-1}$. The force experienced by the pulled terminal residue, F is defined as $F(t) = k(vt - x)$ where, x is the displacement of the pulled atom from its original position, v is the pulling velocity, and k is the spring constant. The direction of pulling was such that the end-to-end distance always increased, *i.e.*, the SMD residue was pulled away from the fixed residues.

Analysis:

Analysis of the trajectories, including finding number of H-bonds were done by GRO-MACS 5.1 [32]. Base-pair orientation parameters and stacking geometry were analysed by NUPARM [41–43].

III. RESULTS ANALYSIS

We first look at the stability of the equilibrium MD simulation. Previous equilibrium molecular dynamics studies by several groups had observed that separation of the strands of siRNA took place during interaction with graphene or carbon nanotube [44–48]. It was also demonstrated that such separation of strands did not happen in case of double stranded DNA[45, 46], thus attributed this siRNA separation to specific interaction between carbon nanomaterial and siRNA. Our recent study, however indicate siRNA remains in double helical form in physiological environment [34]. This indicates that external force is possibly needed to compel the separation of strands in siRNA. The results compliments our equilibrium simulations, which also demonstrates only moderate RNA breathing in equilibrium

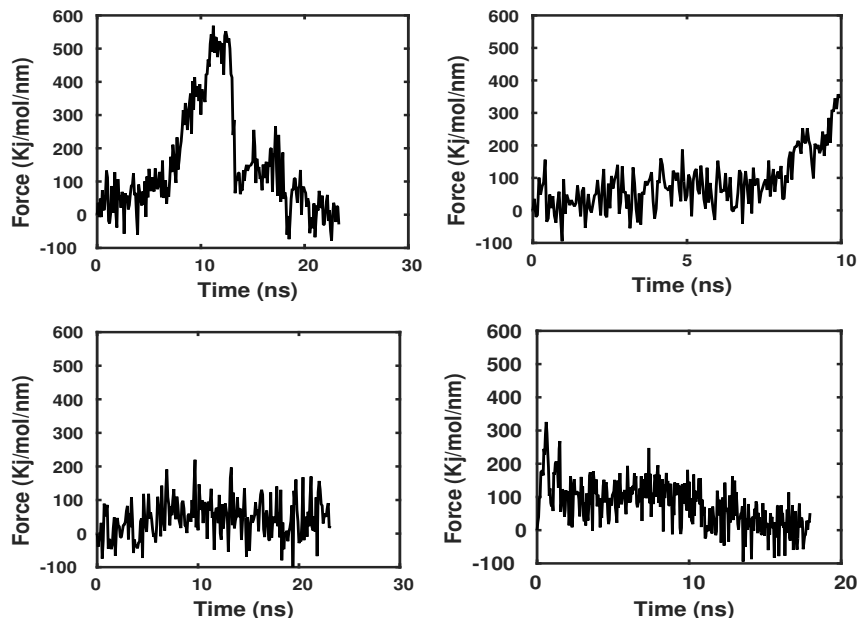


FIG. 2: Shows the variation of force experienced by the system with the time under different protocol as shown in Figure 1. (a) Corresponds to the variation of force with time for the Axial Rupture model. (b) Corresponds the variation of force for the pulling of the Axial Stretch model. (c) Corresponds the variation force for the pulling of the Terminal Unzip model and (d) Corresponds the variation force applied for the Central Unzip model of siRNA.

MD throughout the 100 ns production run. We have taken the final equilibrated structure of siRNA duplex from the equilibrium MD simulation for further force induced SMD simulations. In SMD or center of mass (COM) pulling the system is biased to demonstrate the behavior toward a particular phenomenon. Application of an external force to cause displacement in the simulated system allows for the calculation of work, a path-dependent quantity. For opening of the strands of the siRNA we adopted two standard protocols as described in method section (Figure 1), one is to apply force along the helical direction of the system and the other is to apply the force perpendicular to the helical direction of the system, the later can be generalised as unzipping.

We have measured the forces experienced by the siRNA, which vary with time for the different model systems (Figure 2). Figure 2a shows the variation of force with time for the Axial Rupture model. We observe nearly linear variation of extension with simulation time (Figure SI 1), hence the force *vs.* extension curves also look very similar. In the case of Axial Rupture one strand is pulled along helical axis direction keeping the far end of the other strand constrained. During the initial phase of pulling, the 3'-terminal single stranded UU residues adopt stretched out conformation, which does not require any extra effort. The double helical structure is also not affected by such conformational change of the single stranded region. After this phase, varying peaks of the curve reveal that structural transition occurs and the system starts to change from its double-helical form. One expects the hydrogen bonds (H-bonds) between the complementary bases to break at this moment. The stacking interactions between successive base-pairs also may get affected during this second phase of simulation with large force. The third option is that both take place simultaneously during this phase. In order to understand the mechanism, we have analysed number of H-bonds present in the system at each time frame (Figure 3). Total number of H-bonds continue to decrease with time in the first phase, *i.e.* upto 10 ns (Figure 3a, blue curve). After about 10 ns, the number of H-bonds do not reduce significantly with time, possibly indicating most of the phase transitions took place by 10 ns. However, the number of H-bonds in the double helix does not reduce to zero value within this time. As seen in Figure 2a, the force increases at this point of time when number of H-bonds between the two strands appear to increase slightly. After this phase transition, number of H-bonds slowly reduces to zero when the strands dissociate completely (Figure 3a, blue line). But, after this critical interaction the system breaks and the requirement of an additional force starts to decrease. In this time duration, force reduction from maximum to minimum reveals the structural change of the system from the bound double helical state to the completely unbound ssRNA state. Both the strands become almost separated, where most of the base-pairs are broken. It may be noted that the unfolded single stranded chains has capability to form intra strand H-bonds and hence, the blue line does not reach to zero value. This can

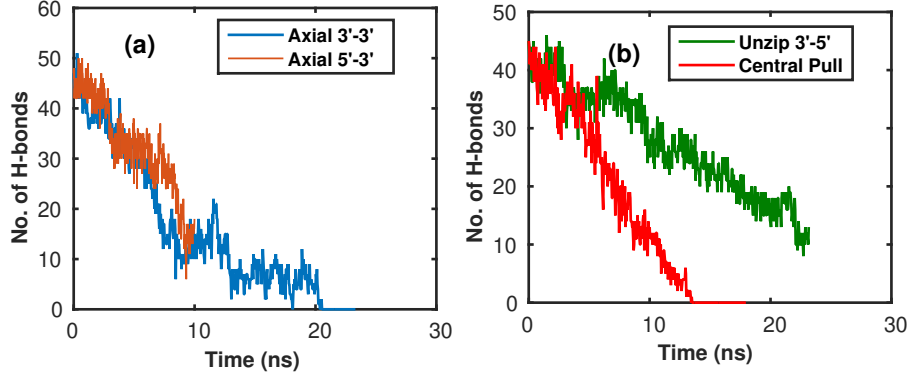


FIG. 3: Variation of number of H-bonds in between the two strands of siRNA with time during (a) Axial Rupture (blue line) and Axial Stretch (yellow line) SMD simulations and (b) Terminal Unzip (green line) and Central Unzip (red line) SMD simulations.

be visualised by the various snapshots shown in the first row of Figure 4.

Variation of force with time for the Axial Stretch model system is shown in Figure 2b, where the constrained point and pulling end are on the same strand and pulling is done along the helical direction (Figure 1b) somewhat similar to the Axial Rupture model. Variation of force with time, however, is found to differ significantly from that of Axial Rupture model. Here, slight increase in the force during the last phase of SMD simulation is presumably due to conformational transition of the pulled strand to somewhat all-trans geometry, which is obviously not energetically favorable, especially for nucleic acids [49]. Nevertheless, in this case completely separated strands do not arise because pulling is done on the strand which is also fixed at the other end. But, it is noticeable that, even then force induced breakage of most of the base-pair H-bonds between the complementary strands take place (yellow line in Figure 3a). This can also be visualised by the snapshots shown in second row of Figure 4. The helical structure is converted to ladder like form (Figure 4), but most of the bases remain close to their complementary ones of the opposite strand. Thus, some H-bonds were retained till the end of the SMD simulation and further pulling was impossible as that would need to break or stretch the covalent bonds. Possible such effort took place after around 8

ns, showing increase in the measured force.

Variation of unzipping force with time for the Terminal Unzip model system is shown in Figure 2c. Here, unzipping starts from one end and propagates to the far side progressively. This kind of strand separation was also observed by several groups in MD simulations of dsDNA at elevated temperature [50–52] or partially even at physiological condition. This can be termed as extension of fraying or peeling effect. In this case intact base-pairs are breaking gradually and progressively one by one, which causes the system to experience almost equal small force in steps until complete separation of the strand. And hence, variation of force is nearly at constant small value at all time steps. The progression of simulation can be seen by the different snapshots shown in first row of Figure 5. The base-pairs break continuously as time progresses, which is also reflected in number of H-bonds (Figure 3b, green curve). Significant reduction of number of H-bonds was not observed till 8 ns, as the single stranded UU residues were changing to stretched out conformation during this phase.

We observe unique result on the Central Unzip model system (Figure 1d), where force is also applied perpendicular to the helical direction of the RNA but in this case at the central residue (11th residue) of one of the strands keeping the paired residue of the complementary strand immobile. Here, also the variation of force experienced by the system with time is qualitatively similar to that of terminal-unzip model system. However, it is notable that the measured force is significantly larger (nearly $300 \text{ kJ mol}^{-1} \text{ nm}^{-1}$) in the initial phase (Figure 2d) as compared to the other systems. After the initial phase the force reduces to smaller magnitude around $100 \text{ kJ mol}^{-1} \text{ nm}^{-1}$ and even smaller values. This initial increase of force can be explained as initiation of base-pair opening and the later as propagation of base pair opening to both sides of the central one. This is equivalent to nucleation energy for cooperative transition from helix to coil state. The nucleation energy is quite high, as it would disrupt a base pair (at least two hydrogen bonds) and two stacking interactions between the pulled base pair and its two neighboring base-pairs on both sides. The second type of force is supposedly stronger than the base pairing energy and it is doubled also [53]. Once the H-bonds of the central base-pair break and the stacking between the central

base-pair and its neighbouring base-pair are disrupted, the neighbouring base-pairs can have fraying like effect. In other word these neighbouring base-pairs come to contact with solvent water. Hence, These bases can form H-bond with the complementary bases or with solvent water molecules in a competitive manner. The trajectory of this model system can be visualised by the snapshots shown in the second row of Figure 5. Furthermore, the propagation stage is quite faster as compared to the other SMD results, as two base-pairs break together, *i.e.*, C+1 and C-1 after base pair C breaks (where C is the central base-pair) then C+2 and C-2 break and so on. Hence, they can now easily become single stranded breaking the Watson- Crick base pairing and stacking interactions, requiring small amount of force.

IV. STRUCTURAL TRANSITION

As indicated above, the H-bonds between the complementary bases in a base-pairs breaks during force induced SMD simulations. Thus the bases do not remain coplanar to each other and the other degrees of freedom of the bases also increase beyond their regular values. Quantitative analysis of these degrees of freedom of the bases with respect to paired ones can be done by the six IUPAC-IUB recommended intra base-pair parameters [54]. We have therefore looked at shear, open angle and stretch values, which are related to the H-bonding features. Similarly relative orientations of a base-pairs with respect to their neighbouring stacked ones also change significantly when the stacking interactions are disrupted. These can be analysed by tilt, roll, etc., inter base-pair local parameters. Effect of all these inter base-pair parameters can also be analysed by a composite parameter, namely stacking overlap, and we have analysed that also. Variation of shear, base-pair overlap and twist, as representative parameters, are shown in Figure 6 and Figure 7 to compare all the systems.

The shear parameter gives information about relative movement of the bases with respect to the paired ones, indicating disruption of hydrogen bonds in a base pair, overlap provides information about stacking between two base-pairs and twist indicates ladder like structure

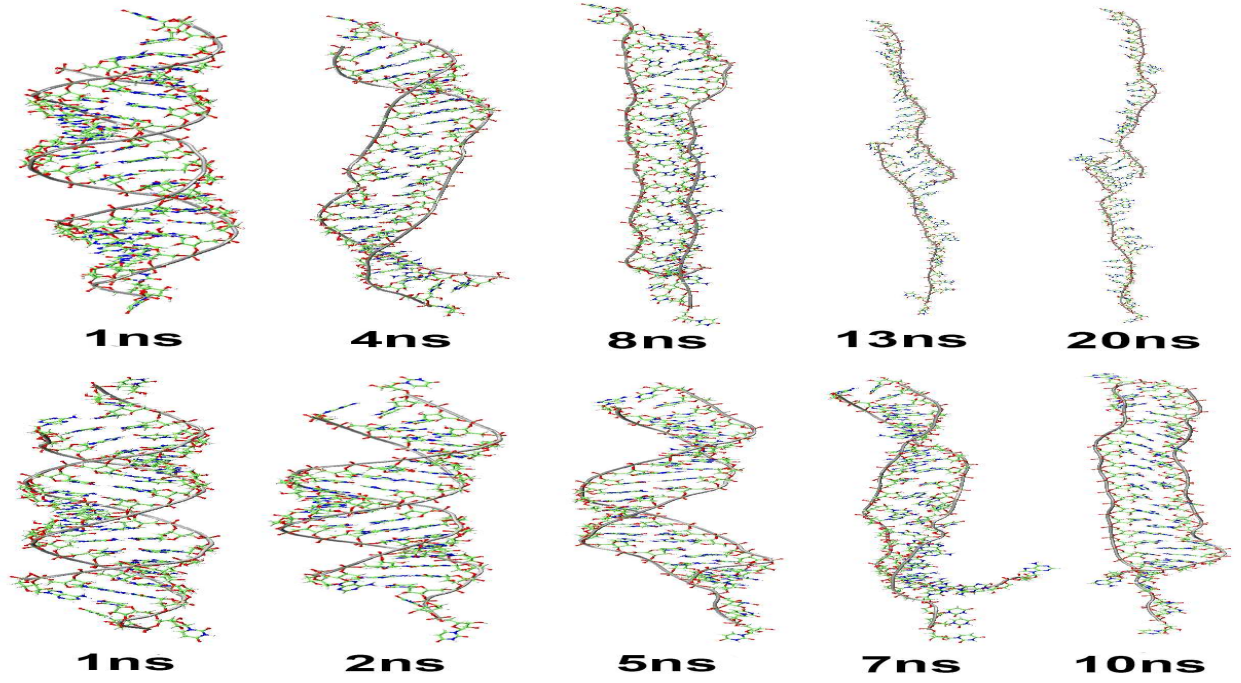


FIG. 4: Panel of axial force application: First row corresponds to the snapshots of structural transition for Axial Rupture model system. Second row corresponds to the snapshots of structural transition for the Axial Stretch model system.

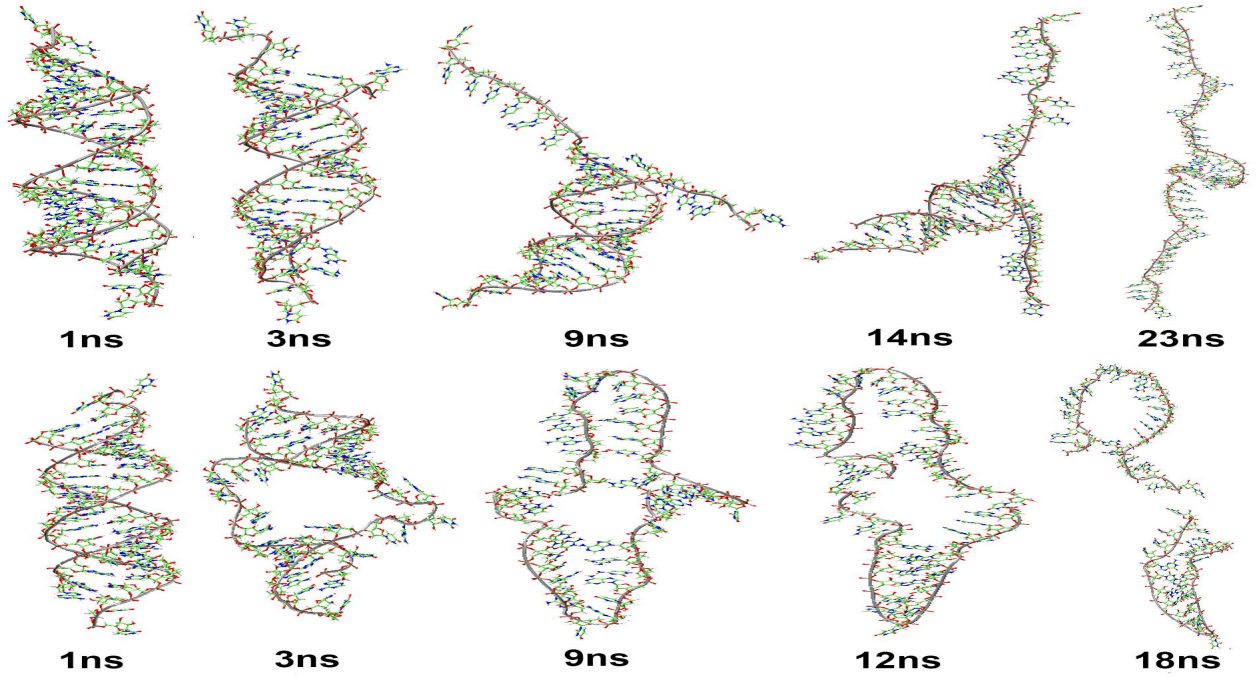


FIG. 5: Panel of force applied to the unzipping model systems: First row corresponds the snapshots of structural transition for the Terminal Unzip model system. Second row corresponds the snapshots of structural transition for the Central Unzip model system.

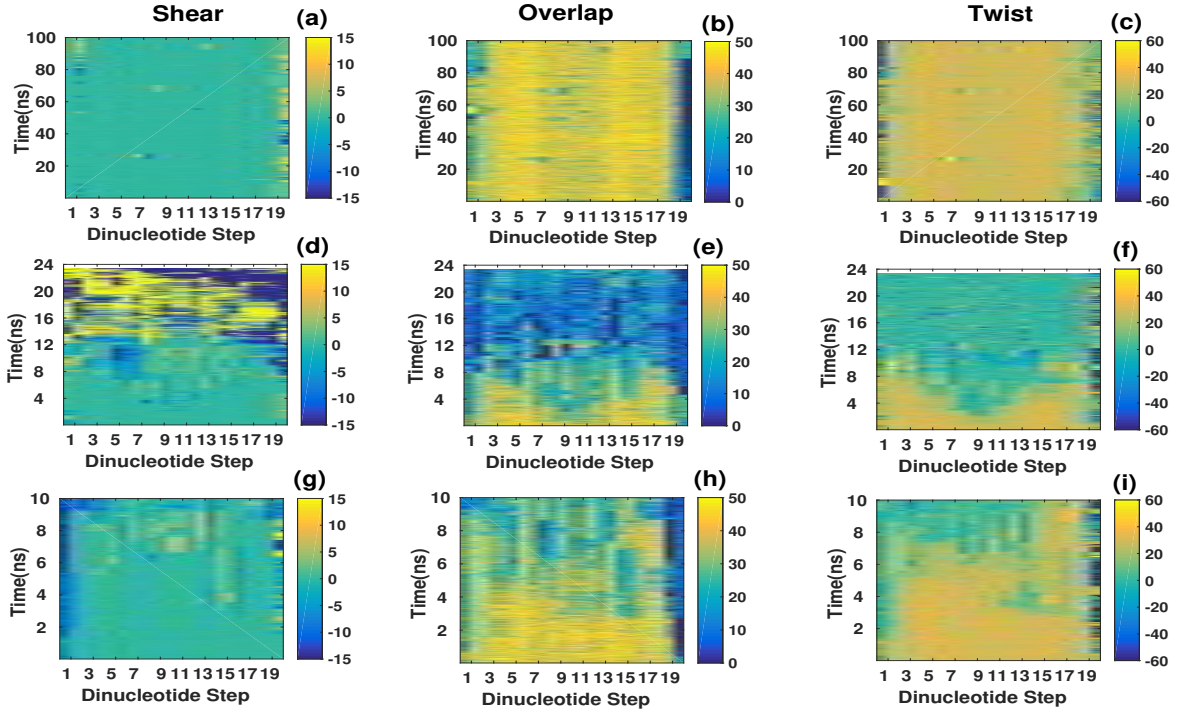


FIG. 6: Variation of base pair parameters during equilibrium and axial pulling simulations. Residue numbers are shown in x-axis, time in y-axis and the graded color for values of (a) shear (\AA), (b) overlap (\AA^2) and (c) twist ($^\circ$), for equilibrium simulation. The shear, overlap and twist for Axial Rupture model are shown in (d), (e) & (f) while (g), (h) & (i) are the same for Axial Stretch.

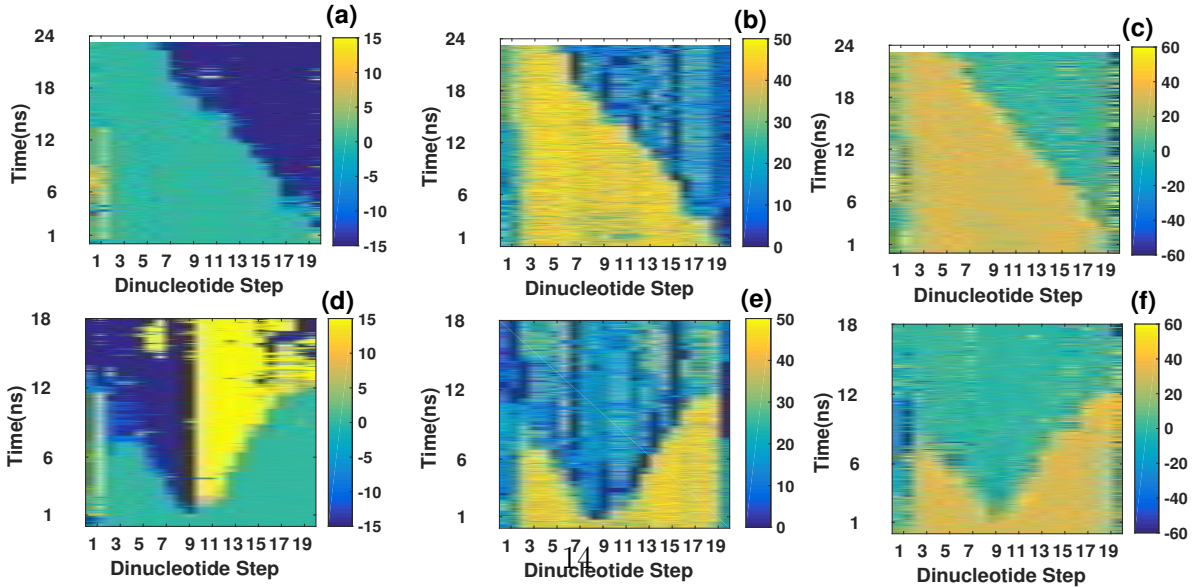


FIG. 7: Base pair parameters for unzipping SMD simulations. The base-pair numbers are shown in x-axis, time (ns) in y-axis and the graded color represents values of: (a) shear (\AA), (b) overlap

formation, and hence is often related to stretching [21]. These are illustrated as three dimensional plots. It may be noted that shear values of good Watson-Crick base-pairs are around zero [42], twist value of A-RNA stretches are around 33° [49] and stacking overlap between successive base-pairs in RNA double helices are around 45 to 50 \AA^2 [43] depending on base sequence. We have also analyzed variation of these parameters during equilibrium MD simulations of the siRNA to understand the force induced effects on the double helical structure (Figure 6a, b & c). From the figures, it is clear that the structure maintains almost ideal values of these parameter throughout the simulation, indicating that no separation of the strands took place in absence of any force or molecules like graphene or carbon nanotube. Furthermore, terminal fraying is also found to be minimum as compared to other simulations using CHARMM force-field [52], possibly due to somewhat capping effect by the two single stranded residues at the two ends of the double helix.

The changes in the parameters for the Axial Rupture system are shown in Figure 6d, e & f. Figure 6d illustrates that initially upto 4 ns shear values of all the 20 base-pairs are near 0 (sky blue color), indicating no disruption of any base-pair. After that minor disruption of base pairing can be seen with minor fluctuation of shear values until 10 ns. Here, the shear values of 5th, 6th and 7th base-pairs become more negative and can be seen to be more affected by the force. Base-pairs of 5'-terminal residue adopt large positive shear and all the base-pairing near 3'-terminal assume large negative shear. All the shear values start changing because of structural transition after 12 ns and afterwards huge fluctuation of shear (Yellow color corresponding to values around $10 - 15 \text{ \AA}$ or deep blue color for shear values around -15 \AA) indicate disruption of initial base pairing. Comparing with disruption of H-bonds (Figure 3a for Axial Rupture model) it can be concluded that, after breaking half of the total possible H-bonds (from ≈ 48 to 25) the disruption is steep linear after around 12 ns. Variation of overlap parameters (Figure 6e) illustrates continuous disruption of stacking for all the base-pair steps within 8 ns, and it is seen to initiate after 2 ns at the central region. However, even at this time (8 ns) most of the bases are paired to their complementary ones, as reflected from the analysis of shear. Thus, base-pairs opening and

stacking disruption appear to be independent and unrelated events. For few instances, we found that, after complete breakdown of the stacking, again overlap value increases due to single stranded helix like structure formation. Such single stranded structure formation leads to stacking between successive bases, instead of stacking between successive base-pairs in double-stranded RNA. From Figure 6f it appears that the twist values of the base-pairs at different helical positions start to fluctuate at diverse time points. The middle base pair steps (9th and 10th) faces twist disruption at as early as 2 ns. Comparing with the two other parameters, shear and overlap, we found twist to get disrupted earliest and become most sensitive to the applied force. It is noted that the central base-pairs are getting effected earlier possibly due to weaker base-pairing in the central region (AU rich sequence). These structural transitions can be seen with snapshots throughout the simulation in first row of Figure 4.

Structural parameter variations for the Axial Stretch model of same strand pulling are presented by Figure 6g, h & i. Interestingly, it can be observed that in this case values of the parameters have complete different signature of variation as compared to the Axial Rupture model. We found that the regular shear variation is maintained for much longer time of pulling for all the base-pairs as compared to Axial Rupture model (Figure 6d). However, somewhat larger fluctuation of shear values is observed for few base-pairs (14th to 17th) after 4 ns. These base-pairs are also seen to be unstacked with respect to their neighbours from 4 ns (Overlap values reduce to around 20 \AA^2). As expected twist value of these base-pairs also reduce at the same time. Disruption in stacking overlap is also found less for Axial Stretch model system (Figure 6h) as compared to Axial Rupture model system (Figure 6e). Even at the end of Axial Stretch model simulation significant stacking overlap around 30 \AA^2 is found between successive base-pairs, indicating separation of the strands did not take place. Comparing with the breaking of H-bonds for this case (Figure 3a, yellow line) showing that even after the system is melted the number of H-bonds are still significant (> 10 number), which can be observed by different snapshots shown in second row of Figure 5. We find twist values (Figure 6i) are sensitive to the force as compared to shear and overlap in Axial

Stretch model. However, the fluctuation starts late as compared to Axial Rupture model. These differences in variations can be related to lesser disruption of H-bonds in Figure 3a for axial-stretch model, indicating the situation that complete force induced rupture is not taking place.

Variations of base pair parameter for Terminal Unzip model system are shown in Figure 7a, b & c. In this case the fixed end and the end at which pulling force is applied are on the same terminal side of the duplex and this unzipping mode is prominent in the signature of parameter variations. Variation of shear (Figure 7a) indicates that the disruptions of base-pairs are completely dependent on the base positions. The terminal to the pulling end is first disrupted by the unzipping force, which starts to perturb the system from the pulling end gradually (19th base pair). Similar gradual disruption of overlap values can be observed from Figure 7b. This illustrates that the unzipping effect are progressive in nature and minimal effect is transmitted to the bases far from the current unzipped base pair. This is almost equivalent to extension of fraying effect seen earlier [52].

Shear variation for the Central Unzip (Figure 7d), clearly indicates melting of the central base pair occurs just after 1 ns. The base-pairs next to the central pulled one (12th one) acquire large positive shear, while previous one (10th base pair) gets large negative shear and this feature continuous till the end. The base-pairs, which are away from the pulling point, maintain almost same value (near zero, cyan color) for much longer time. Similar structural changes can be observed in terms of stacking overlap value for all base positions as shown in Figure 7e. The overlap values of the 6th residue and 14th residue appear to increase to value close to 35 \AA^2 after 7 ns, indicating formation of secondary helix-loop-helix like structure within the separated single strands. This can be visualized by the snapshots (at 9 ns, 12 ns and 18 ns) in lower panel of Figure 5. In terms of variation of twist value (Figure 7f) similar trend of separation of the strands starting from central pulling positions is observed.

V. DISCUSSION

In this study, we have tried to integrate structural transition of the system with different protocols of applied force. We found that, when pulling is applied at the axial direction (Axial Rupture) of the system, it experiences highest force compared to all other protocols. In this case highest force ($\sim 600 \text{ kJ mol}^{-1} \text{ nm}^{-1}$) builds up to a point until certain critical interaction is broken. On the other hand, for the same direction pulling (Axial Stretch) the force continuously increases because the fixed end and pulled end are situated at the same strand. Nevertheless, ultimate disruption of most of the H-bonds in this case indicates that separation of the strands can also be achieved by this way of steering. In case of pulling perpendicular to the helix axis, the system unzips in usual way of strand separation. Here, opening of base-pairs are progressive and is achieved one by one from the pulling terminal. Due to this, during initial simulation time, force increases and then maintains almost same value over the pulling time. Among the protocols of pulling, Central Unzipping looks most different as compared to others. In this case, initially system experiences strong force, because of opening of first intact base-pairs and simultaneously unstacking the central base pair from both the sides of pulled nucleotides. But, eventually successive opening of progressive H-bonds requires much less force compare to all other cases of pulling. This is also revealed by the measurement of breaking of number of H-bonds. Hence this mode of opening can be viewed as most feasible as compared to all other possible protocols of siRNA strand separation.

We have also looked at the crystal structures of RNA double helical fragments bound to argonaute protein from Protein Data Bank [56] to evaluate the most interactive structural signature of RNA. We found the protein bound double helical RNA strands are of significant length (10 or more base-pairs) in 3HJF, 3HK2, 3HM9, 4N47, 4NCB, 5AWH and 5UXO. We have analyzed hydrogen bonds between the protein and RNA using PyrHBfind software [57] and have focused on the strong ones. The middle portion of the RNA duplex is found to be mostly interacting with protein residues by formation of very strong H-bonds involving

negatively charged phosphate group of RNA and positively charged Lys or Arg residues of argonaute. In most of the cases, one of the ends of each strand is also found similarly anchored. e.g. 3HJF.pdb [55] and 3HK2.pdb [55] have length of double helical region are 12 and 14 respectively and around 3 to 4 bases of both the strand residing at the middle region of the helix in total forms H-bonds with the Protein. Hence, accepting the idea that more crowding will enable higher grip by protein and subsequently lead to rupture start-point, we can conclude that, central pulling must be most feasible phenomena in nature. However, crowding at one of the terminals may indicate that other mechanisms could also take place, though with lesser probability. The complete understanding of anchoring the siRNA at multiple points (center as well as the terminals) may require new methodological development to analyze the system. Again, the role of UU overhang cannot be detected in the unzipping of siRNA duplex, which might be involved in some other process. Among the helical parameters, we observed that for all the case of pulling, twist parameter is most sensitive during the opening of strands of siRNA duplex. Experimental determination of siRNA structure in Protein Data Bank is so far inadequate in number. In future perspective, it is necessary to study the effects different sequences and length for the system of siRNA and observe the changes associated.

VI. ACKNOWLEDGEMENTS

We gratefully acknowledge SERB and DST, New Delhi India for their financial supports through project numbers PDF/2015/000308 and PDF/2017/002110/CS. We also acknowledged CDAC for their computing support. Most of the simulations were performed in the cluster of CAPP-II project of DAE. We thank Prof. Sanjay Kumar of Banaras Hindu Univer-

sity and Prof. Rituparna Sinharoy of IISER-Kolkata for discussion and useful suggestions.

- [1] Fire, A., Xu, S., Montgomery, M.K., Kostas, S.A., Driver, S.E. and Mello, C.C. (1998) Potent and specific genetic interference by double-stranded RNA in *Caenorhabditis elegans*. *Nature*, **391**, 806-811.
- [2] Dogini, D.B., Pascoal, V.D.A.B., Avansini, S.H., Vieira, A.S., Pereira, T.C. and Lopes-Cendes, I. (2014) The new world of RNAs. *Genet. Mol. Biol.*, **37**, 285-293.
- [3] Sashital, D.G. and Doudna, J.A. (2010) Current Opinion in Structural Biology. *Curr. Opin. Struct. Biol.*, **20**, 90-97.
- [4] Martinez, J., Patkaniowska, A., Urlaub, H., Lhrmann, R., Tuschl, T. (2002) Single-stranded antisense siRNAs guide target RNA cleavage in RNAi. *Cell*, **110**, 563-74.
- [5] Meister, G. and Tuschl, T. (2004) Mechanisms of gene silencing by double-stranded RNA. *Nature*, **431**, 343-9.
- [6] Li, J., Xue, S. and Mao, Z.W. (2016) Nanoparticle delivery systems for siRNA-based therapeutics. *J. Mater. Chem. B*, **4**, 6620-6639.
- [7] Wu, S. Y., Lopez-Berestein, G., Calin, G.A. and Sood, A.K. (2014) RNAi therapies: drugging the undruggable. *Sci. Transl. Med.*, **6**, 240.
- [8] Davidson, B.L. and Jr. McCray, P.B. (2011) Current prospects for RNA interference-based therapies. *Nat. Rev. Genet.*, **12**, 329-40.
- [9] Fellmann, C. and Lowe, S.W. (2014) Stable RNA interference rules for silencing. *Nat. Cell Biol.*, **16**, 10-18.
- [10] Kumar, S., Jensen, I., Jacobsen, J.L. and Guttamann A.J. (2007) Role of conformational entropy in force-induced biopolymer unfolding. *Phys. Rev. Lett.*, **98**, 128101.
- [11] Kumar, S. and Li, M.S. (2010) Biomolecules under mechanical force. *Phys. Rep.* **486**, **1**, 1-74.
- [12] Essevaz-Roulet, B., Bockelmann, U. and Heslot, F. (1997) Mechanical separation of the complementary strands of DNA. *Proc. Natl. Acad. Sci. USA*, **94**, 11935-11940.

- [13] U. Bockelmann, Essevaz-Roulet, B. and Heslot, F. (1997) Molecular Stick-Slip Motion Revealed by Opening DNA with Piconewton Forces. *Phys. Rev. Lett.*, **79**, 4489.
- [14] Strunz, T., Oroszlan, K., Schäfer, R. and Güntherodt, H.J. (1999) Dynamic force spectroscopy of single DNA molecules. *Proc. Natl. Acad. Sci. USA*, **96**, 11277-82.
- [15] Schumakovitch, I., Grange, W., Strunz, T., Bertoncini, P., Güntherodt, H.J. and Hegner, M. (2002) Temperature dependence of unbinding forces between complementary DNA strands. *Biophys. J.*, **82**, 517-521.
- [16] Danilowicz, C., Kafri, Y., Conroy, R.S., Coljee, V.W., Weeks, J. and Prentiss, M. (2004) Measurement of the Phase Diagram of DNA Unzipping in the Temperature-Force Plan. *Phys. Rev. Lett.*, **93**, 078101.
- [17] Hatch, K., Danilowicz, C., Coljee, V. and Prentiss, M. (2008) Demonstration that the shear force required to separate short double-stranded DNA does not increase significantly with sequence length for sequences longer than 25 base pairs. *Phys. Rev. E*, **78**, 011920.
- [18] Danilowicz, C., Limouse, C., Hatch, K., Conover, A., Coljee, V.W., Kleckner, N. and Prentiss, M. (2009) The structure of DNA overstretched from the 5'5' ends differs from the structure of DNA overstretched from the 3'3' ends. *Proc. Natl. Acad. Sci. USA*, **106**, 13196-13201.
- [19] Kühner, F., Morfill, J., Neher, R.A., Blank, K. and Gaub, H.E. (2007) Force-Induced DNA Slippage. *Biophys. J.*, **92**, 2491-2497.
- [20] Cocco, S., Monasson, R. and Marko, J.F. (2001) Force and kinetic barriers to unzipping of the DNA double helix. *Proc. Natl. Acad. Sci. USA*, **98**, 8608-8613.
- [21] Marin-Gonzaleza, A., Vilhenaa, J.G., Perezb, R. and Moreno-Herreroa, F. (2017) Understanding the mechanical response of double-stranded DNA and RNA under constant stretching forces using all-atom molecular dynamics. *Proc. Natl. Acad. Sci. USA*, **114**, 7049-7054.
- [22] Herrero-Galán, E., Fuentes-Perez, M.E., Carrasco, C., Valpuesta, J.M., Carrascosa, J.L., Moreno-Herrero, F. and Arias-Gonzalez, J.R. (2013) Mechanical Identities of RNA and DNA Double Helices Unveiled at the Single-Molecule Level. *J. Am. Chem. Soc.*, **135**, 122.
- [23] Lipfert, J. Skinner, G.M. *et al.* (2014) Double-stranded RNA under force and torque: Sim-

- ilarities to and striking differences from double-stranded DNA. *Proc. Natl. Acad. Sci. USA*, **111**, 15408-413.
- [24] Mandal, M., Lee, M. Barrick, J.E., Weinberg, Z., Emilsson, G.M., Ruzzo, W.L., Breaker, R.R. (2004) A glycine-dependent riboswitch that uses cooperative binding to control gene expression. *Molecu. Bio.*, **306**, 275-279.
- [25] Chandra, V. Hannan, Z., Xu, H. and Mandal, M. (2017) Single-molecule analysis reveals multi-state folding of a guanine riboswitch. *Nature Chem. Biol.*, **13**, 194-201).
- [26] Savinov, A., Perez, C.F. and Blockc, S.M. (2014) Single-molecule studies of riboswitch folding. *Biochim. Biophys. Acta.*, **1839**, 1030-1045.
- [27] Gupta, A. and Bansal. M. (2017) The Role of Sequence in Altering the Unfolding Pathway of an RNA Pseudoknot: A Steered Molecular Dynamics Study. *Phys. Chem. Chem. Phys.*, **18**, 28767-28780.
- [28] Zuo, Y. and Steitz, T.A. (2015) Crystal Structures of the E. coli Transcription Initiation Complexes with a Complete Bubble *Molecular Cell*, **58**, 534-540.
- [29] Mallick Gupta, A., Mukherjee, S., Dutta, A., Mukhopadhyay, J., Bhattacharyya, D. and Mandal, S. (2017) Identification of a suitable promoter for the sigma factor of Mycobacterium tuberculosis. *Mol. BioSystems* **13**, 2370-2378.
- [30] Saecker, R.M., Record Jr, M.T. and deHaseth, P.L. (2011) Mechanism of Bacterial Transcription Initiation: RNA Polymerase - Promoter Binding, Isomerization to Initiation-Competent Open Complexes, and Initiation of RNA Synthesis *J. Mol. Biol.* **412**, 754-771.
- [31] Yuan, Y.R., Pei, Y., Chen, H.Y., Tuschl, T., and Patel, D.J. (2006) A Potential Protein-RNA Recognition Event along the RISC-Loading Pathway from the Structure of A. aeolicus Argonaute with Externally Bound siRNA. *Structure* **14**, 1557-1565.
- [32] Abraham, M.J., Murtola, T., Schulz, R., Pall, S., Smith, J.C., Hess, B. and Lindahl, E. (2015) GROMACS: High performance molecular simulations through multi-level parallelism from laptops to supercomputers. *SoftwareX*, **1-2**, 19-25.
- [33] Best, R.B., Zhu, X., Shim, J., Lopes, P.E.M., Mittal, J., Feig, M. and MacKerell, A.D. (2012)

- Optimization of the Additive CHARMM All-Atom Protein Force Field Targeting Improved Sampling of the Backbone ψ , and Side-Chain χ^1 and χ^2 Dihedral Angles. *J. Chem. Theory Comput.*, **8**, 3257-3273.
- [34] Biswas, A., Chakraborty, K., Dutta, C., Mukherjee, S., Gayen, P., Jan, S., Mallick, A.M., Bhattacharyya, D. and Sinha Roy, R. (2019) Engineered Histidine-Enriched Facial Lipopeptides for Enhanced Intracellular Delivery of Functional siRNA to Triple Negative Breast Cancer Cells. *ACS Appl. Mater. and Interfaces*, **11**, 4719-4736.
- [35] Berendsen, H.J.C., Postma, J.P.M., van Gunsteren, W.F., DiNola, A. and Haak, J.R. (1984) Molecular dynamics with coupling to an external bath. *J. Chem. Phys.*, **81**, 3684.
- [36] Nosé, S. (1984) A unified formulation of the constant temperature molecular dynamics methods. *J. Chem. Phys.*, **81**, 511.
- [37] Hoover, W.G. (1985) Canonical dynamics: Equilibrium phase-space distributions. *Phys. Rev. A*, **31**, 1695.
- [38] Nosé, S., Klein, M.L. (1983) Constant pressure molecular dynamics for molecular systems. *Mol. Phys.*, **50**, 1055-1076.
- [39] Parrinello, M. and Rahman, A. (1981) Polymorphic transitions in single crystals: A new molecular dynamics method. *J. Appl. Phys.*, **52**, 7182.
- [40] Darden, T., York, D. and Pedersen, L. (1993) Particle mesh Ewald: An Nlog(N) method for Ewald sums in large systems. *J. Chem. Phys.*, **98**, 10089.
- [41] Bansal, M., Bhattacharyya, D. and Ravi, B. (1995) NUPARM and NUCGEN: software for analysis and generation of sequence dependent nucleic acid structures. *Bioinformatics*, **11**, 281-287.
- [42] Mukherjee, S., Bansal, M. and Bhattacharyya, D. (2006) Conformational specificity of non-canonical base pairs and higher order structures in nucleic acids: crystal structure database analysis. *J. Comput. Aided Mol. Des.*, **20**, 629-45.
- [43] Pingali, P.K, Halder, S, Mukherjee, D., Basu, S. Banerjee, R. Choudhury, D. and Bhattacharyya, D. (2014) Analysis of stacking overlap in nucleic acid structures: algorithm and

- application. *J. Comput. Aided Mol. Des.*, **28**, 851-867.
- [44] Jung, S., Cha, M., Park, J., Jeong, N., Kim, G., Park, C., Ihm, J. and Lee, L. Dissociation of Single-Strand DNA: Single-Walled Carbon Nanotube Hybrids by WatsonCrick Base-Pairing. *J. Am. Chem. Soc.*, **132**, 10964-10966.
- [45] Santosh, M., Panigrahi, S., Bhattacharyya, D., Sood, A. K. and Maiti, P. K. (2012) Unzipping and binding of small interfering RNA with single walled carbon nanotube: a platform for small interfering RNA delivery. *J. Chem. Phys.*, **136**, 065106.
- [46] Santosh, M., Panigrahi, S., Bhattacharyya, D., Sood, A.K. and Maiti, P.K. (2012) Unraveling siRNA unzipping kinetics with graphene. *J. Chem. Phys.*, **137**, 054903.
- [47] Landry, M.P., Vukovic, L., Kruss, S., Bisker, G., Landry, A.M., Islam, S., Jain, R., Schulten, K. and Strano, M.S. (2015) Comparative Dynamics and Sequence Dependence of DNA and RNA Binding to Single Walled Carbon Nanotubes. *J. Phys. Chem. C.*, **119**, 10048-10058.
- [48] Ghosh. S. and Chakrabarti, R. (2016) Spontaneous Unzipping of Xylonucleic Acid Assisted by a Single-Walled Carbon Nanotube: A Computational Study. *J. Phys. Chem. B.*, **120**, 3642-3652.
- [49] Needle, S., Schneider, B., and Berman, H.M. *Structural Bioinformatics*, 2nd ed (P.E. Bourne, H. Weissig, eds), pp.41-76 (2009).
- [50] Wong, K.Y. and Pettitt, B.M. (2008) The Pathway of Oligomeric DNA Melting Investigated by Molecular Dynamics Simulations. *Biophys. J.*, **95**, 5618-5626.
- [51] Zgarbova, M., Otyepka, M., Sponer, J., Lankas, F. and Jurecka, P. (2014) Base Pair Fraying in Molecular Dynamics Simulations of DNA and RNA. *J. Chem. Theory Comput.*, **10**, 3177-3189.
- [52] Kundu, S., Mukherjee, S. and Bhattacharyya. D. (2017) Melting of polymeric DNA double helix at elevated temperature: a molecular dynamics approach. *J. Mol. model*, **23**, 226.
- [53] Yakovchuk, P., Protozanova, E. and Frank-Kamenetskii, M.D. (2006) Base-stacking and base-pairing contributions into thermal stability of the DNA double helix. *Nucl. Acids Res.*, **34** , 564-574.
- [54] Olson, W.K., Bansal, M., Burley, S.K., Dickerson, R.E., Gerstein, M., Harvey, S.C., Heine-

- mann, U., Lu, X.J., Neidle, S., Shakked, Z., Sklenar, H., Suzuki, M., Tung, C.S., Westhof, E., Wolberger, C. and Berman, H.M. (2001) A standard reference frame for the description of nucleic acid base-pair geometry. *J. Mol. Biol.* **313**, 229-237.
- [55] Wang, Y., Juranek, S., Li, H., Sheng, G., Wardle, G.S., Tuschl, T. and Patel, D.J. (2009) Nucleation, propagation and cleavage of target RNAs in Ago silencing complexes. *Nature*, **461**, 754-761.
- [56] Berman, H.M., Westbrook, J., Feng, Z., Gilliland, G., Bhat, T.N., Weissig, H., Shindyalov, I.N., Bourne, P.E. (2000) The Protein Data Bank. *Nucl. Acids Res.* **28**, 235-252.
- [57] Mukherjee, S., Majumdar, S. and Bhattacharyya, D. (2005) Role of Hydrogen Bonds in Protein-DNA Recognition: Effect of Nonplanar Amino Groups. *J. Phys. Chem. B* **109**, 10484-10492.